Evidence of active role played by the nonmagnetic element Sr in magnetostructural coupling in $SrRuO_3$

Debdutta Lahiri,[1,*,†] T. Shibata,[2,3] S. Chattopadhyay,[2,3] Sudipta Kanungo,[4] T. Saha-Dasgupta,[4,*,‡] R. S. Singh,[5] Surinder M. Sharma,[1] and Kalobaran Maiti[5,*,§]

[1]*High Pressure and Synchrotron Radiation Physics Division, Bhabha Atomic Research Centre, Trombay, Mumbai 400085, India*

[2]*BCPS Department, Illinois Institute of Technology, Chicago, Illinois 60616, USA*

[3]*CSRRI-IIT, MRCAT, Advanced Photon Source, Sector 10, Argonne, Illinois 60439, USA*

[4]*Advanced Materials Research Unit, S.N. Bose National Center for Basic Sciences, JD Block, Sector III, Salt Lake City, Kolkata 700098, India*

[5]*Department of Condensed Matter Physics and Materials Science, Tata Institute of Fundamental Research, Homi Bhabha Road, Colaba, Mumbai 400005, India*

(Received 11 June 2010; revised manuscript received 8 August 2010; published 24 September 2010)

We study the magnetic transition in $SrRuO_3$, the only itinerant 4*d* ferromagnet, employing x-ray absorption fine structure study and *state-of-the-art* band-structure calculations. Both experimental and theoretical results reveal an unusual evolution of the local structural parameters around the spectator element, Sr, across the magnetic transition. Interestingly, such evolution of the Sr-related bonds nucleate at a temperature, $T^{\star}$, higher than the magnetic transition temperature, indicating the presence of a precursor effect. Contrary to common belief, these results point to the active role played by the Sr ion in the magnetostructural coupling present in this compound.

DOI: 10.1103/PhysRevB.82.094440 PACS number(s): 75.30.Kz, 61.05.cj, 61.50.Ks, 71.15.Mb

I. INTRODUCTION

Perovskite structured oxides of general formula ABO_3 attracted a great deal of attention followed by the discovery of exotic properties such as high-temperature superconductivity, giant magnetoresistance, etc.[1] The crystal structure of $SrRuO_3$ forming in perovskite derived structure is shown in Fig. 1. The electronic and magnetic properties of these compounds are determined by the BO_6 units shown by the shaded units in the figure. The *A*-site elements, sitting in the void between corner-shared BO_6 units are generally believed to provide cohesion in the lattice without direct involvement in the properties of the material. Recent studies of 4*d* transition-metal oxides such as ruthenates, however, apparently exhibit exception to this common belief. For example, $SrRuO_3$ is the only ferromagnetic 4*d* transition metal oxide (T_C=165 K) (Ref. 2) despite the fact that Ru possesses similar correlation-induced moment in all its composites.[3] On the other hand, a similar compound, $CaRuO_3$ does not show long-range ferromagnetic order[4–6] and exhibit possible non-Fermi-liquid behavior.[7–9]

Evidently, the observation of varied magnetic ground state in ruthenates does not follow the conventional wisdom that attributes the role of nonmagnetic ions such as Sr, Ca located at *A* sites as spectators. The conventional wisdom, though seems justified from the perspective of electronic structure; the alkaline earths at *A* sites contribute negligibly to the density of states at the Fermi level, ϵ_F.[4,10,11] Thus, the anomalous experimental observation appears apparently puzzling. Recent band-structure calculations[4] and x-ray photoemission study,[11] however, indicate significant covalency between *A*-site elements and oxygen that introduces orthorhombic distortions.[12] It, therefore, seems natural to *A*-O covalency and consequent changes in the structural parameters to be linked to their varied physical properties observed in these systems which needs attention.[13,14] The magnetovolume effect[15] observed in $SrRuO_3$ and not in $CaRuO_3$ points to a definite role of structure on magnetism in these compounds.

In this paper, we study the evolution of the structural parameters of $SrRuO_3$ and associated disorder as a function of temperature using x-ray absorption fine structure (XAFS) study.[16] Element specificity of XAFS makes it best suited to resolve the structures selectively around different atoms, viz., magnetic Ru and nonmagnetic Sr. We corroborate our experimental findings in terms of *state-of-the-art* band-structure calculations. Our XAFS results exhibit anomalous thermal evolution of Debye-Waller factors (DWFs) associated to Sr-related bonds across the magnetic transition. The structural

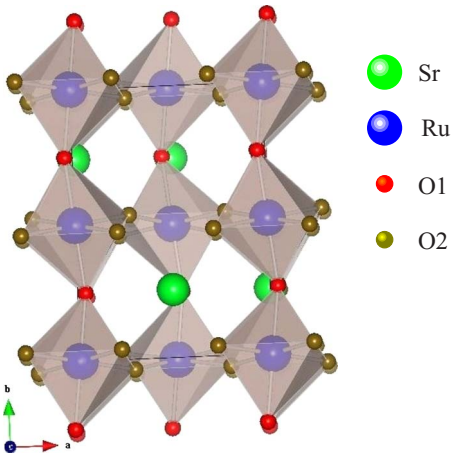

FIG. 1. (Color online) Crystal structure of $SrRuO_3$ forming in perovskite structure. RuO_6 units are shown by shaded octahedra. Sr atoms which sit in the hollow formed by corner-shared RuO_6 units, are shown by big circles. The oxygen atoms at the apical positions of the RuO_6 octahedra are labeled as O1 and those at the plane are labeled as O2.

evolution for individual RuO_6 octahedra, on the other hand, is found to follow the usual trend expected due to thermal expansion/contraction without showing any anomalous behavior across the magnetic transition. This is in contrast to the previous observations of magnetoelastic effects and distortion-mediated magnetic transitions in various other compounds, all involving the magnetic ions.[17,18] Interestingly, such thermal evolution nucleates at a temperature, $T^{\star}$ higher than the Curie temperature revealing a possible *precursor effect*.

The remainder of the paper is organized as follows. Section II includes the details of the experimental measurements carried out in this study. In Sec. III, we present the methodology and the details of the computations carried out in this study. Section IV describes our obtained results along with the discussions. Section V provides the conclusion.

II. EXPERIMENTAL DETAILS

High-quality sample of $SrRuO_3$ was prepared in the polycrystalline form following solid-state reaction route as described elsewhere.[19] Good crystalline quality was confirmed by x-ray diffraction (XRD) and various bulk measurements. For example, the magnetic susceptibility measurements exhibit a ferromagnetic transition at 165 K, the highest found so far in various studies using samples both in single crystalline and polycrystalline forms. This establishes good quality of the sample. In order to perform XAFS measurements, the sample was further ground to 5 μm particle size and pasted on scotch tape. XAFS data at Sr *K* edge (16.105 keV) and Ru *K* edge (22.117 keV) were collected at the undulator beamline of MRCAT (Materials Research Collaborative Access Team), Advanced Photon Source, USA.[20] The temperature-dependent measurements (10–300K) were performed in transmission using a Displex cryostat. The data were processed using ATHENA and the structural parameters were fit using FEFF8 and FEFFIT packages.[21]

III. CALCULATIONAL DETAILS

The structural optimization was carried out in the presence and absence of magnetism in terms of nonspin-polarized and spin-polarized calculations using the plane-wave-based pseudopotential framework of density-functional theory (DFT) as implemented in Vienna *ab initio* simulation package (VASP).[22] The exchange-correlation functional was chosen to be that of generalized gradient approximation. The optimized geometries were obtained by full relaxation of the atomic positions and the lattice constants. The spin-orbit interaction at Ru site was included in the calculations in scalar relativistic form as a perturbation to the original Hamiltonian. The positions of the ions were relaxed toward equilibrium until the Hellmann-Feynman forces become less than 0.001 eV/Å. We used projected augmented wave[23] potentials and the wave functions were expanded in the plane-wave basis with kinetic-energy cutoff of 500 eV. Reciprocal-space integration was carried out with a k mesh of $6\times6\times6$. A k mesh of $6\times6\times6$ gives rise to 64 k points in the irreducible part of the Brillouin zone, which was found to be sufficient to achieve convergence.

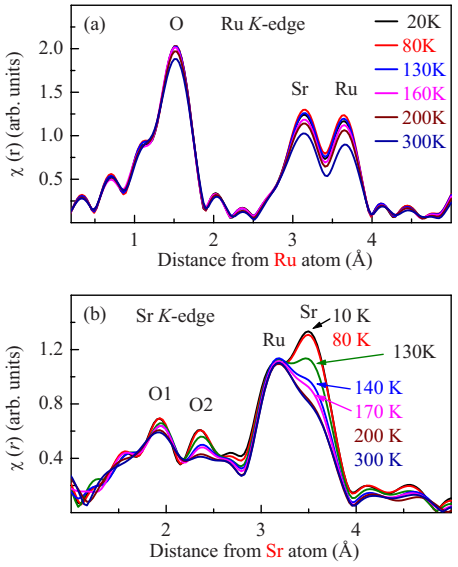

FIG. 2. (Color online) Fourier transform of the k^2-weighted XAFS data at different temperatures at (a) Ru *K* edge and (b) Sr *K* edge.

The Wannier functions were computed using the down-folding technique within the framework of muffin-tin orbital (MTO) based *N*th-order MTO (NMTO) (Ref. 24) method. The reliability of the calculations in the plane-wave and muffin-tin orbital basis sets has been cross-checked.

IV. RESULTS AND DISCUSSIONS

The Fourier transform of the k^2-weighted XAFS data, $\chi(r)$ at Ru, and Sr *K* edges are shown in Fig. 2. To reduce the uncertainties in fit parameters, the data sets for different temperatures were fit simultaneously constraining the coordination number for each bond to be common between the data sets. Other parameters, viz., bond length and DWF were allowed to vary.[25] All the fits showed excellent fit quality (*R* factor <0.005).[21] In Fig. 2(a), we observe that the peaks at Ru *K* edge increases gradually with the decrease in temperature. However, those at Sr *K* edge shown in Fig. 2(b) exhibits anomalous temperature evolution. Most notable changes are observed in the vicinity of 3.5 Å. Moving from high temperature to low temperature, the spectral function at 200 K is found to be almost identical to the one at 300 K indicating no change in structural parameters within this temperature range. The spectral function begins to change below 200 K, changes being most significantly across the magnetic transition. This is evident by comparing the changes in spectral functions between 140 and 130 K, and those between 200 and 300 K and between 80 and 10 K.

The Ru-O bond parameters and DWFs were best fit for k^1-weighted Fourier transforms of the Ru *K*-edge data over the range of 2.5–13 $Å^{-1}$. The derived Ru-O bond lengths as well as DWFs are shown in Fig. 3(a). The Ru-O bond length does not exhibit significant change with temperature, the average values being about 1.945 Å, the small increase may be

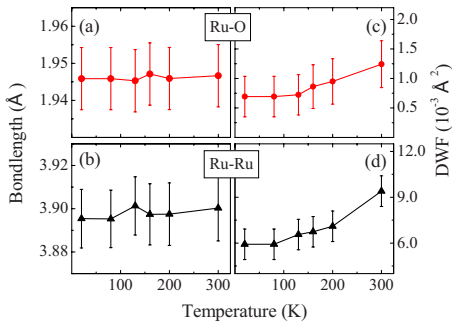

FIG. 3. (Color online) Temperature dependence of the bond lengths (left column) and corresponding Debye-Waller factors (right column) for the structural units around Ru sites.

related to the thermal expansion. The DWF corresponding to Ru-O bonds are shown in Fig. 3(c), which show a very low static value. Increase in temperature leads to a small and gradual rise in magnitude of DWF demonstrating rigidity of the Ru-O octahedra.

The higher shell peaks at Ru *K* edge include contributions from (i) Ru-Sr scattering appearing between 2–3 Å, (ii) Ru-Ru and Ru-O-Ru multiple-scattering (MS) contributions appearing between 3–4 Å. For fitting MS paths, their bond lengths and coordination number were parametrized for angular dependence.[14,26] The result corresponding to Ru-Ru bond length is shown in Fig. 3(b), the temperature-induced effect is very similar to that observed in Fig. 3(a). Interestingly, the static value of the Ru-Ru DWF shown in Fig. 3(d) (Ref. 27) is larger than that of Ru-O bonds.

The results obtained from Sr *K*-edge data are shown in Fig. 4. The immediate neighborhood around Sr consists of a wide distribution of O atoms at different bond lengths between 2.45 and 3.11 Å. This is reflected as bimodal distribution [e.g., O1 and O2 in Fig. 2, where O1 and O2 are

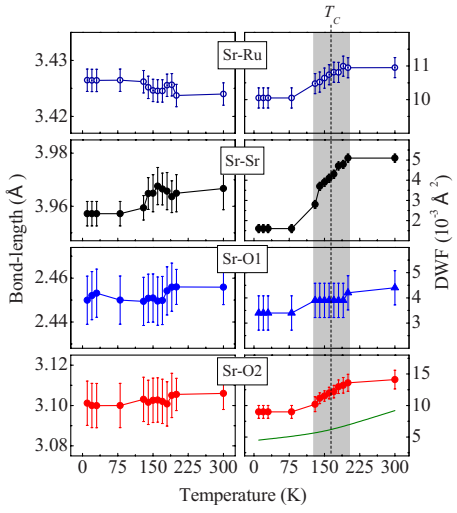

FIG. 4. (Color online) Temperature dependence of the bond lengths (left panel) and corresponding DWF (right panel) for the structural units around the Sr site. The solid line in the bottom-most right panel represents the calculated Debye-Waller factor from correlated Debye model corresponding to the Debye temperature of 525 K.

out-of-plane and in-plane oxygen (see Fig. 1) of the RuO_6 octahedra, respectively] in the Fourier-transformed XAFS data. The neighbors farther out are Ru and Sr. The O and Sr/Ru parameters were best fit for k^1- and k^3-weighted Fourier transforms of the Sr *K*-edge data over the *k* range 3.2–12.5 Å^{-1}.[28]

The results at Sr *K* edge are shown in Fig. 4. The thermal evolution of the bond lengths shown in the left panel of Fig. 4, though nonmonotonic, is negligible (within the uncertainties of the analysis). On the other hand, the Debye-Waller factors shown in the right panel of Fig. 4 evolve significantly with temperature. This brings out the essential observation of this study. For example, (i) DWF corresponding to all the bonds (Sr-O, Sr-Sr, and Sr-Ru) show anomalous thermal evolution in the sense that all the changes are highly nonmonotonic and occur across a temperature range around T_C as marked by shaded region in Fig. 4. The change is most profound in the case of Sr-Sr bonds. (ii) The thermal evolution of DWF deviate from the standard model of phonon evolution (e.g., correlated Debye Model), as shown by solid line in the bottom-most right panel of Fig. 4. The DWF was calculated using correlated Debye model in FEEF6 and assuming reported values of Debye temperature for this compound. The Debye model captures the thermal phonon contributions (both acoustic and optic modes) in a solid. Thus, a deviation from correlated Debye model suggests important contributions such as Jahn-Teller (JT) distortion, polaron formation, etc., which are beyond the consideration of this model. A similar deviation found in manganites in an earlier study[18] was attributed to the Jahn-Teller type of distortions. While Jahn-Teller type of distortions may be applicable to parameters related to Ru-O bonds, it may be ruled out for Sr-Sr bond. Thus, the deviation from the Debye model observed in the present case, may be attributed to the magnetization-induced changes in the lattice distortions from ideal crystal structure. This deviation, therefore, manifests the importance of Sr in the magnetization of this system.

The relatively less sensitivity of the individual RuO_6 octahedron to the ferromagnetic transition is not unexpected considering the fact that the magnetic moments of $2.7\mu_B$ observed in the paramagnetic phase does not change significantly across the paramagnetic to ferromagnetic transition.[3,5] The "nonmagnetic" Sr atoms, on the other hand, as explained above, are found to be sensitive to the magnetic transition. In order to probe the issue of the importance of Sr in magnetism of this compound further, we have carried out structural optimization in the presence and absence of magnetism in terms of nonspin-polarized and spin-polarized calculations. The covalency[29] between occupied O 2*p* states and the empty Sr *d* states, which drives the $GdFeO_3$ kind of orthorhombic distortion in $SrRuO_3$, pulls each O1(O2) closer to one (two) of its four nearest Sr neighbors. This introduces four nearest neighbors to Sr out of 12 oxygen neighbors in the cubic phase. In addition, the Sr cube gets distorted making one body diagonal shortest. The distortion around Ru, reflected in the differences of Ru-O bond lengths, includes the difference of in plane, Ru-O2 and out of plane, Ru-O1 bond lengths as well as the in-plane Jahn-Teller distortion which makes four of the Ru-O2 bond lengths divided into two groups. In Table I, we list the calculated distortion of

TABLE I. Relative changes in the distortion of Sr-O, Sr-Sr, and Ru-O bonds in absence and presence of ferromagnetism. For details, see Ref. 30.

	Struc. with magn. off (Å)	Struc. with magn. on (Å)	Relative change (%)
Δ(Sr-O1)	0.37	0.33	11.4
Δ(Sr-O2)	0.35	0.31	12.1
$\Delta(\text{Sr-Sr})_{diag}$	0.27	0.29	6
$\Delta(\text{Sr-Sr})_{edge}$	0.07	0.08	13
Δ(Ru-O)	0.01	0.01	0

Sr-O bond lengths, Δ(Sr-O), Sr-Sr bond lengths, Δ(Sr-Sr), and Ru-O bond lengths, Δ(Ru-O) for the optimized geometries obtained in absence and presence of magnetic ordering.[30] It is evident that while the changes in Δ(Sr-O1) and Δ(Sr-O2) are as big as 11–12 % and that of Δ(Sr-Sr) are 6–13 %, the distortion of the RuO_6 octahedra remains unchanged upon switching the magnetism on and off. This clearly supports the experimental observation of the sensitivity of Sr-related parameters upon the magnetic transition.

The covalent bonds in this class of perovskite materials can be visualized by a set of localized Wannier functions for the occupied O 2*p* bands.[29] For this purpose, we used NMTO (Ref. 24) based downfolding technique of the construction of Wannier functions. All the degrees of freedom other than O 2*p*, have been downfolded to arrive at a truly minimal basis set that span only the O 2*p* bands. In Fig. 5, we show the plot of such Wannier functions centered at one of the O2 oxygen in the two optimized geometries; one obtained in absence of magnetism and another in its presence. The central parts of the Wannier functions have the p_y character while the tails exhibit the covalency effect with the neighboring Ru atoms and Sr atoms. The relatively strong covalency effect between 4*d* element Ru and O is seen in tails shaped as Ru t_{2g} residing at two neighboring Ru sites, which remain practically unchanged between two Wannier functions. The tail sitting at the Sr position with shortest O2-Sr bond length, however, shows significant changes in its relative weight between the two Wannier functions (shown by encircled region). It is to be noted here that one should focus on the relative changes rather than the absolute magnitudes. While the magnitude of Ru-O covalency is much larger than that of Sr-O covalency, it is the Sr-O covalency that changes upon switching on the magnetism. The above experimental and theoretical results, put together, clearly suggest the sensitivity of Sr on magnetic transition, the magnetism being sensed well by Sr via a change in Sr-O covalency.

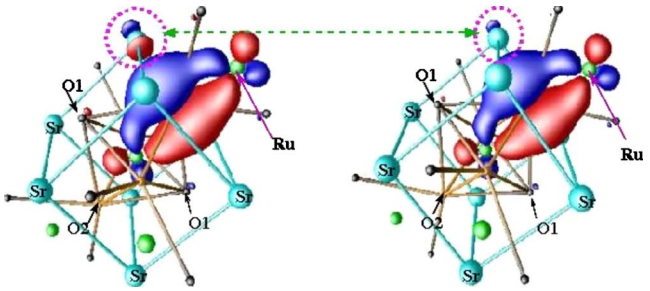

FIG. 5. (Color online) Wannier functions of the minimal set of O 2*p* NMTOs calculated for optimized geometries with magnetization off (left panel) and magnetization on (right panel). The orbital shapes (constant amplitude surfaces) with ± signs are labeled by red and blue colors, respectively.

The importance of O 2*p* *A*-site *d* covalency in determining the $GdFeO_3$ kind of distortions often observed in the ABO_3 structure was predicted long ago by Goodenough.[31] An extensive series of semiempirical simulations carried out during last two decades supported this hypothesis.[12,29,32] *Ab initio* calculations for $SrRuO_3$ also showed that Sr-O covalency plays a significant role in determining the Ru-O-Ru bond angle and the $GdFeO_3$ kind of distortion that the crystal structure experiences.[4] The intersite magnetic coupling between Ru atoms depends on Ru-O-Ru exchange path that helps electrons to hop from one site to the other and to couple Ru moments. Therefore, the intersite exchange coupling, which is a sensitive function of Ru-O-Ru bond angle, is expected to be influenced by the Sr-O covalency. Indeed, the DFT optimization shows Ru-O-Ru angle to change by about 3° upon switching on the magnetism. Individual RuO_6 octahedra, on the other hand, plays the role of magnetic centers and not the mediator of intersite magnetic couplings, and presumably, therefore, is insensitive to the magnetic ordering. One would, though, expect this change in Ru-O-Ru angle to be reflected in other Ru-related structural parameters in some way. As mentioned earlier, the peak between 3–4 Å in Ru *K*-edge spectra has contribution from (i) Ru-Ru single scattering and (ii) Ru-O-Ru double scattering, etc. Though the large intrinsic uncertainties (~8°) in angular variation in backscattering factor for small angles prohibits the extraction of thermal variation in Ru-O-Ru angle directly from XAFS data, the larger values of Ru-Ru DWF compared to Ru-O DWF hints to this effect.

Further examination of Fig. 4 brings out another interesting point. The magnetism-dependent structural evolution nucleates already at a temperature about 200 K (the right edge of the shaded part in Fig. 4), higher than the ferromagnetic T_C of 165 K, hinting to a precursor behavior. The observation of such precursor effect associated to various phase transitions (e.g., the signature of ground electronic states such as electron pairs in the case of superconductors,[33] short-range order in the case of magnetic systems,[34] pseudogap phase) is a widely discussed topic in the recent day research. Although numerous studies are available in the literature on

this topic, the origin of pseudogap phase and/or the temperature, $T^{\star}$ at which such phase nucleates, is debated. Our results, discover such a scenario in $SrRuO_3$ associated to its magnetic transition, thereby suggesting generic nature of precursor effect associated to various phase transitions and also establishes its link to structural parameters[35] indicating a magnetostructural coupling as has been discussed in the literature before.[10] One may note that the possibility of such anomalous behavior arising from multiple phases leading to multiple T_C's is ruled out, both from magnetic, XRD measurements and extended x-ray-absorption fine structure (EXAFS) fitting.[36]

V. CONCLUSIONS

In summary, we investigated the structural evolution across the magnetic transition in $SrRuO_3$ employing XAFS and band-structure calculations. The Debye-Waller factors calculated from the experimental spectra reveal important role of the nonmagnetic Sr ion in the magnetic transition in contrast to the conventional wisdom attributing such effects only to the magnetic ions. This conclusion is consistent with the results obtained independently from the state-of-the-art *ab initio* band-structure calculations. This finding indicates that the magnetostructural coupling is mediated by the Sr ion, which normally one would expect to play the role of a spectator. Furthermore, this interesting phenomenon is found to occur with the precursor effect associated with the magnetic phase transition.

ACKNOWLEDGMENTS

MRCAT operations were supported by the Department of Energy and MRCAT host institutions. Usage of the Advanced Photon Source was supported by the U.S. Department of Energy, Office of Science, Office of Basic Energy Sciences, under Contract No. DE-AC02-06CH11357.

*Corresponding author.
†debdutta.lahiri@gmail.com
‡tanusri@bose.res.in
§kbmaiti@tifr.res.in

[1] A. Georges, G. Kotliar, W. Krauth, and M. J. Rozenberg, Rev. Mod. Phys. **68**, 13 (1996); M. Imada, A. Fujimori, and Y. Tokura, *ibid.* **70**, 1039 (1998).
[2] J. J. Randall and R. Ward, J. Am. Chem. Soc. **81**, 2629 (1959); A. Callaghan, C. W. Moeller, and R. Ward, Inorg. Chem. **5**, 1572 (1966); J. M. Longo, P. M. Raccah, and J. B. Goodenough, J. Appl. Phys. **39**, 1327 (1968).
[3] M. Takizawa, D. Toyota, H. Wadati, A. Chikamatsu, H. Kumigashira, A. Fujimori, M. Oshima, Z. Fang, M. Lippmaa, M. Kawasaki, and H. Koinuma, Phys. Rev. B **72**, 060404(R) (2005); K. Maiti and R. S. Singh, Phys. Rev. B **71**, 161102(R) (2005).
[4] K. Maiti, Phys. Rev. B **73**, 235110 (2006); **77**, 212407 (2008).
[5] G. Cao, S. McCall, M. Shepard, J. E. Crow, and R. P. Guertin, Phys. Rev. B **56**, 321 (1997).
[6] P. Khalifah, I. Ohkubo, H. M. Christen, and D. G. Mandrus, Phys. Rev. B **70**, 134426 (2004).
[7] L. Klein, L. Antognazza, T. H. Geballe, M. R. Beasley, and A. Kapitulnik, Phys. Rev. B **60**, 1448 (1999).
[8] K. Maiti, R. S. Singh, and V. R. R. Medicherla, EPL **78**, 17002 (2007).
[9] G. Cao, O. Korneta, S. Chikara, L. E. DeLong, and P. Schlottmann, Solid State Commun. **148**, 305 (2008).
[10] D. J. Singh, J. Appl. Phys. **79**, 4818 (1996).
[11] R. S. Singh and K. Maiti, Phys. Rev. B **76**, 085102 (2007).
[12] E. Pavarini, S. Biermann, A. Poteryaev, A. I. Lichtenstein, A. Georges, and O. K. Andersen, Phys. Rev. Lett. **92**, 176403 (2004).
[13] Y. He, P. Sharma, K. Biswas, E. Z. Liu, N. Ohtsu, A. Inoue, Y. Inada, M. Nomura, J. S. Tse, S. Yin, and J. Z. Jiang, Phys. Rev. B **78**, 155202 (2008); E. Eisenberg and R. Berkovits, Ann. Phys. **8**, 707 (1999); M. Berciu and R. N. Bhatt, Phys. Rev. Lett. **87**, 107203 (2001); A. H. Slobodskyy, V. K. Dugaev, and M. Vieira, Condens. Matter Phys. **5**, 531 (2002); A. Semwal and S. N. Kaul, Pramana, J. Phys. **60**, 513 (2003); K. Potzger, S. Zhou, Q. Xu, A. Shalimov, R. Groetzschel, H. Schmidt, A. Mücklich, M. Helm, and J. Fassbender, Appl. Phys. Lett. **93**, 232504 (2008); S.-R. Eric Yang and A. H. MacDonald, Phys. Rev. B **67**, 155202 (2003).
[14] D. Haskel, E. A. Stern, D. G. Hinks, A. W. Mitchell, J. D. Jorgensen, and J. I. Budnick, Phys. Rev. Lett. **76**, 439 (1996); D. Haskel, E. A. Stern, F. Dogan, and A. R. Moodenbaugh, Phys. Rev. B **61**, 7055 (2000); D. Lahiri, Physica C **436**, 32 (2006); T. Shibata, B. A. Bunker, and J. F. Mitchell, Phys. Rev. B **68**, 024103 (2003); T. Shibata, B. Bunker, J. F. Mitchell, and P. Schiffer, Phys. Rev. Lett. **88**, 207205 (2002).
[15] T. Kiyama, K. Yoshimura, K. Kosuge, Y. Ikeda, and Y. Bando, Phys. Rev. B **54**, R756 (1996).
[16] R. Prins and D. C. Koningsberger, *X-Ray Absorption: Principles, Applications, Techniques of EXAFS, SEXAFS and XANES* (Wiley, New York, 1987).
[17] V. G. Harris, K. D. Aylesworth, B. N. Das, W. T. Elam, and N. C. Koon, Phys. Rev. Lett. **69**, 1939 (1992); S. Pascarelli, M. P. Ruffoni, A. Trapananti, O. Mathon, G. Aquilanti, S. Ostanin, J. B. Staunton, and R. F. Pettifer, *ibid.* **99**, 237204 (2007); R. Macovez, J. Luzon, J. Schiessling, A. Sadoc, L. Kjeldgaard, S. van Smaalen, D. Fausti, P. H. M. van Loosdrecht, R. Broer, and P. Rudolf, Phys. Rev. B **76**, 205111 (2007); D. E. Fowler and J. V. Barth, *ibid.* **53**, 5563 (1996); L. Downward, F. Bridges, S. Bushart, J. Neumeier, N. Dilley, and L. Zhou, Phys. Rev. Lett. **95**, 106401 (2005).
[18] Y. Jiang, F. Bridges, L. Downward, and J. J. Neumeier, Phys. Rev. B **76**, 224428 (2007).
[19] R. S. Singh and K. Maiti, Solid State Commun. **140**, 188 (2006).
[20] C. U. Segre, N. E. Leyarovska, L. D. Chapman, W. M. Lavender, P. W. Plag, A. S. King, A. J. Kropf, B. A. Bunker, K. M. Kemner, P. Dutta, R. S. Duran, and J. Kaduk, *Synchrotron Radiation Instrumentation: SRI99: Eleventh US National Confer-*

ence, AIP Conf. Proc. No. 521 (AIP, New York, 2000), p. 419.
[21] A. L. Ankudinov, B. Ravel, J. J. Rehr, and S. D. Conradson, Phys. Rev. B **58**, 7565 (1998); B. Ravel and M. Newville, J. Synchrotron Radiat. **12**, 537 (2005).
[22] G. Kresse and J. Hafner, Phys. Rev. B **47**, 558(R) (1993); **48**, 13115 (1993); **49**, 14251 (1994).
[23] P. E. Blöchl, Phys. Rev. **50**, 17953 (1994).
[24] O. K. Andersen and T. Saha-Dasgupta, Phys. Rev. B **62**, R16219 (2000).
[25] Although, in the following we present our results for both bond lengths and DWFs, the conclusions are based primarily on DWFs since the trend in bond lengths often are masked by the large error bars associated with them.
[26] D. Haskel, Ph.D. thesis, University of Washington, 1998.
[27] Extraction of Ru-Sr and Ru-Ru DWF is complicated by the interference of MS from Ru-O octahedra. Thus, MS path variables were constrained in correlation with those for single scattering cases and parametrized by simulating buckling-angle dependence of such amplitudes in FEFF6 calculations (Ref. 14).
[28] k^1 weighted fit for O shells deemphasized the contribution of Ru peak. k^2-weighted transform resulted in the O peaks lying along the shoulder of the Ru peaks. Ru, Sr shells were fit for k^3 weight in order to deemphasize the contribution/leakage of Sr-O bonds to the Sr/Ru peaks.
[29] E. Pavarini, A. Yamasaki, J. Nuss, and O. K. Andersen, New J. Phys. **7**, 188 (2005).
[30] Δ(Sr-O) were measured by shortening of the shortest Sr-O bonds relative to the average. The $\Delta(\text{Sr-Sr})_{diag}$ is measured by shortening of the shortest Sr-Ru-Sr body diagonal of the Sr cube from the average and $\Delta(\text{Sr-Sr})_{edge}$ is the difference between the shortest and longest Sr-Sr bond lengths along the cube edge. Since DFT optimization minimizes the JT distortion of the RuO_6 octahedra to a negligible amount, Δ(Ru-O) is defined by the difference between Ru-O2 and Ru-O1 bond lengths. The relative change is the change in Δ's between two optimized geometries.
[31] J. B. Goodenough, Prog. Solid State Chem. **5**, 145 (1971).
[32] P. M. Woodward, Acta Crystallogr., Sect. B: Struct. Sci. **53**, 44 (1997).
[33] A. Kanigel, M. R. Norman, M. Randeria, U. Chatterjee, S. Souma, A. Kaminski, H. M. Fretwell, S. Rosenkranz, M. Shi, T. Sato, T. Takahashi, Z. Z. Li, H. Raffy, K. Kadowaki, D. Hinks, L. Ozyuzer, and J. C. Campuzano, Nat. Phys. **2**, 447 (2006).
[34] N. Mannella, W. L. Yang, X. J. Zhou, H. Zheng, J. F. Mitchell, J. Zaanen, T. P. Devereaux, N. Nagaosa, Z. Hussain, and Z.-X. Shen, Nature (London) **438**, 474 (2005).
[35] K. Maiti, R. S. Singh, V. R. R. Medicherla, S. Rayaprol, and E. V. Sampathkumaran, Phys. Rev. Lett. **95**, 016404 (2005); V. R. R. Medicherla, S. Patil, R. S. Singh, and K. Maiti, Appl. Phys. Lett. **90**, 062507 (2007); R. Bindu, K. Maiti, S. Khalid, and E. V. Sampathkumaran, Phys. Rev. B **79**, 094103 (2009).
[36] Possibility of hidden segregating Sr nanoclusters (not detected by XRD) was ruled out by EXAFS fitting.